journal of the mechanical behavior of biomedical materials 152 (2024) 106453

Contents lists available at ScienceDirect

Journal of the Mechanical Behavior of Biomedical Materials

journal homepage: www.elsevier.com/locate/jmbbm

Research Paper

Leaflet remodeling reduces tricuspid valve function in a computational model

Mrudang Mathur [a], Marcin Malinowski [b,c], Tomasz Jazwiec [d], Tomasz A. Timek [b], Manuel K. Rausch [a,e,f,g,*]

[a] Department of Mechanical Engineering, University of Texas at Austin, 204 E Dean Keeton Street, Austin, 78712, TX, United States of America
[b] Division of Cardiothoracic Surgery, Spectrum Health, 221 Michigan Street NE Suite 300, Grand Rapids, 49503, MI, United States of America
[c] Department of Cardiac Surgery, Medical University of Silesia, Katowice, Poland
[d] Department of Cardiac, Vascular and Endovascular Surgery and Transplantology, Medical University of Silesia in Katowice, Silesian Centre for Heart Diseases, Zabrze, Poland
[e] Department of Aerospace Engineering and Engineering Mechanics, University of Texas at Austin, 2617 Wichita Street, Austin, 78712, TX, United States of America
[f] Department of Biomedical Engineering, University of Texas at Austin, 107 W Dean Keeton Street, Austin, 78712, TX, United States of America
[g] Oden Institute for Computational Engineering and Sciences, University of Texas at Austin, 201 E 24th Street, Austin, 78712, TX, United States of America

ARTICLE INFO

Dataset link: https://github.com/SoftTissueBiomechanicsLab/Texas_TriValve.git

Keywords:
Annuloplasty
Repair
Transcatheter
Maladaptation

ABSTRACT

Tricuspid valve leaflets have historically been considered "passive flaps". However, we have recently shown that tricuspid leaflets actively remodel in sheep with functional tricuspid regurgitation. We hypothesize that these remodeling-induced changes reduce leaflet coaptation and, therefore, contribute to valvular dysfunction. To test this, we simulated the impact of remodeling-induced changes on valve mechanics in a reverse-engineered computer model of the human tricuspid valve. To this end, we combined right-heart pressures and tricuspid annular dynamics recorded in an ex vivo beating heart, with subject-matched in vitro measurements of valve geometry and material properties, to build a subject-specific finite element model. Next, we modified the annular geometry and boundary conditions to mimic changes seen in patients with pulmonary hypertension. In this model, we then increased leaflet thickness and stiffness and reduced the stretch at which leaflets stiffen, which we call "transition-λ." Subsequently, we quantified mean leaflet stresses, leaflet systolic angles, and coaptation area as measures of valve function. We found that leaflet stresses, leaflet systolic angle, and coaptation area are sensitive to independent changes in stiffness, thickness, and transition-λ. When combining thickening, stiffening, and changes in transition-λ, we found that anterior and posterior leaflet stresses decreased by 26% and 28%, respectively. Furthermore, systolic angles increased by 43%, and coaptation area decreased by 66%; thereby impeding valve function. While only a computational study, we provide the first evidence that remodeling-induced leaflet thickening and stiffening may contribute to valvular dysfunction. Targeted suppression of such changes in diseased valves could restore normal valve mechanics and promote leaflet coaptation.

1. Introduction

Heart valves have historically been thought of as inert tissues, or "passive flaps" (Williams and Jew, 2004). However, we now know that they are highly sensitive to their mechano-chemical environment and are "active tissues" (Muresian, 2009; Rausch et al., 2012). In fact, their extra-cellular matrices are populated by valve interstitial cells (VIC) that maintain tissue homeostasis (Meador et al., 2020a). To this end, VICs continually secrete matrix proteins – namely collagen and elastin – and matrix remodeling enzymes to repair tissue and ensure matrix durability (Gupta and Grande-Allen, 2006; Pant et al., 2018). However, VICs may also acquire a hyper-contractile and myofibroblast-like phenotype in response to injury or disease (Wang et al., 2014). These "activated" VICs may drive excess collagen deposition in the extra-cellular matrix. This fibrotic tissue remodeling leads to tissue thickening and stiffening and alters the nonlinearity of their constitutive response. In turn, these tissue-level changes alter the mechanics of valve leaflets (van Kelle et al., 2019; Loerakker et al., 2016). Notably, such changes were reported in the mitral valves of patients

* Corresponding author at: Department of Aerospace Engineering and Engineering Mechanics, University of Texas at Austin, 2617 Wichita Street, Austin, 78712, TX, United States of America.
E-mail address: manuel.rausch@utexas.edu (M.K. Rausch).

https://doi.org/10.1016/j.jmbbm.2024.106453
Received 28 July 2023; Received in revised form 23 January 2024; Accepted 31 January 2024
Available online 2 February 2024

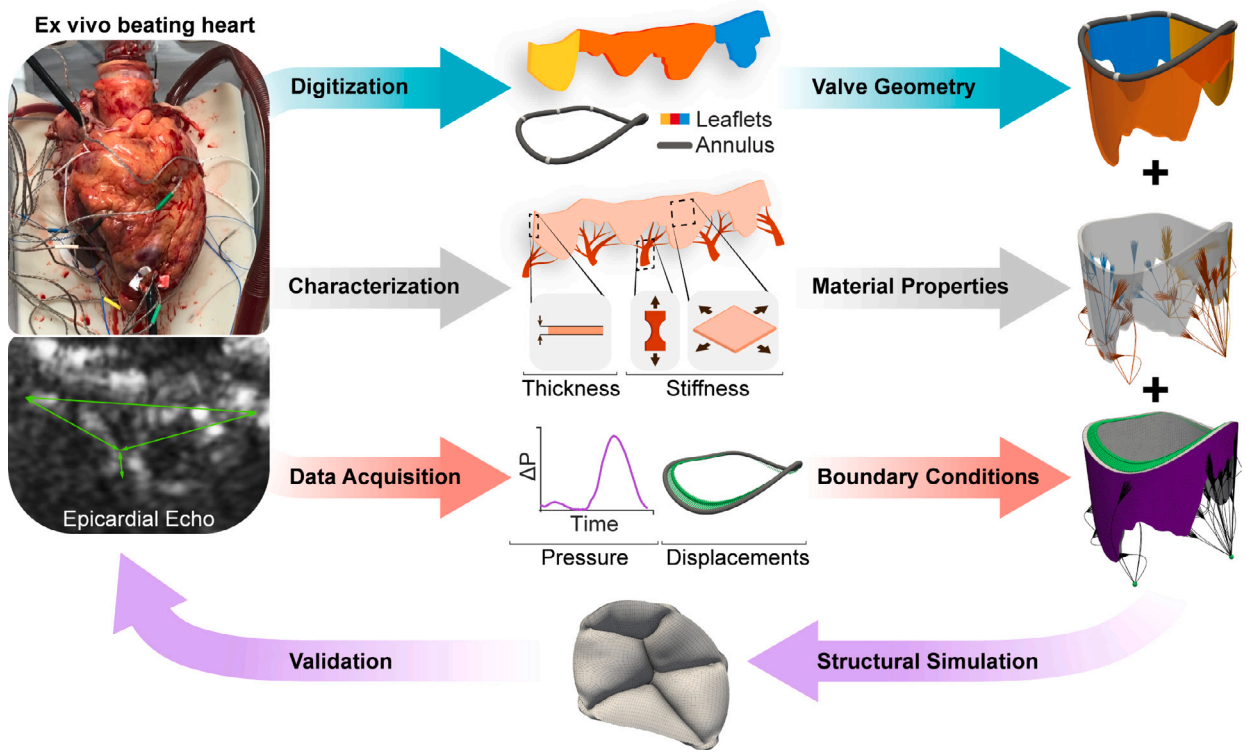

Fig. 1. Texas TriValve 1.0 modeling pipeline. We reverse-engineered a subject-specific computational model of a healthy, human tricuspid valve. To this end, we recorded annular dynamics, transvalvular pressures, and echo images of the tricuspid valve in an ex-vivo beating heart. We then arrested the heart, digitized the valve morphology, and characterized tissue material properties in-vitro. Next, we combined the subject-specific geometry, material properties, and boundary conditions in a finite element model of the valve. Finally, we simulated leaflet coaptation through structural simulations in Abaqus/Explicit and validated our results against echo images of the tricuspid valve in the same beating heart. *Source:* Reproduced with permission from Mathur et al. (2022).

with functional mitral regurgitation (Grande-Allen et al., 2005), where remodeling-induced leaflet thickening and stiffening increased leaflet stresses and reduced coaptation (Kunzelman et al., 1998).

Inspired by these findings, we sought to determine if the tricuspid valve remodels similarly in response to disease — namely, functional tricuspid regurgitation. Moderate to severe tricuspid regurgitation affects nearly 1.6 million patients in the US and is an independent predictor of morbidity and mortality (Nath et al., 2004; Wang et al., 2019). In most cases, the origin of regurgitation is extrinsic to the valve and occurs as a consequence of other pathologies, e.g. pulmonary hypertension, that induce right-ventricular remodeling (Badano et al., 2013). In turn, right-ventricular remodeling leads to annular dilation and papillary muscle displacement that prevent leaflet coaptation. As such, the valve leaflets are thought to remain unaffected and the regurgitation is considered "functional" in nature (Muraru and Badano, 2022). Interestingly, we found evidence of leaflet remodeling in sheep with functional tricuspid regurgitation (Meador et al., 2020b; Iwasieczko et al., 2023). As in the mitral valve, we found leaflet thickening and stiffening and alterations in the material nonlinearity of the leaflets' constitutive response. Additionally, we and others found that tricuspid leaflets grow in area (Afilalo et al., 2015). We hypothesize that these remodeling-induced changes fundamentally alter the leaflets' ability to bend and stretch, thereby affecting valve mechanics. This, in turn, may prevent the enlarged leaflets from sealing the dilated tricuspid orifice; thus impeding valve function. Furthermore, we posit that suppressing these changes in tricuspid leaflets will, in fact, restore valve mechanics and promote leaflet coaptation. The objective of our current study is to test this hypothesis.

2. Methods

2.1. High-fidelity finite element model

To test our hypothesis we use Texas TriValve 1.0, a reverse-engineered and openly accessible computer model of a healthy human tricuspid valve, see Fig. 1. Briefly, we first loaded the right side of a healthy, beating human donor heart in an organ preservation system (OCS, TransMedics, Andover, MA) (Malinowski et al., 2019). In the beating heart, we then recorded transvalvular hemodynamics via miniaturized pressure sensors (PA4.5- X6; Konigsberg Instruments Inc., Pasadena, CA), recorded tricuspid annulus dynamics via sonomicrometry crystals (Sonometrics Inc., London, Ontario, Canada) (Mathur et al., 2019), and imaged tricuspid valve coaptation via epicardial echocardiography (Vivid S6, GE Healthcare, Chicago, IL). Upon arresting the heart, we excised the tricuspid valve complex, digitized the leaflet geometry, and characterized the tissue material properties via in vitro experiments. To rebuild the valve in silico, we non-rigidly warped the digitized leaflet geometry onto a sonomicrometry-based 3D reconstruction of the tricuspid annulus. Next, we created chordal insertion sites based on in vitro images of the leaflets. We then assigned subject-specific hyperelastic material properties to the leaflets and chordae tendineae; informed by planar biaxial and uniaxial tensile tests, respectively. In our model, we then imposed annular displacement and transvalvular pressure gradient boundary conditions based on sonomicrometry crystal and pressure sensor measurements, respectively. Finally, we simulated leaflet coaptation in Abaqus/Explicit (6.20-1, Dassault Systémes, Vélizy-Villacoublay, France) and validated our model deformations against echocardiography images of the tricuspid valve in the same beating heart. Detailed descriptions of model creation and validation are provided in our previous work (Mathur et al., 2022).

In this validated model, we modify annular geometry and boundary conditions to reflect changes seen in patients with pulmonary hypertension, which we refer to as our baseline model (Afilalo et al., 2015). Specifically, we non-uniformly dilate the tricuspid annulus to increase annular area by 62% (Ring et al., 2012), see Fig. 2. Moreover, we tether the papillary muscles and apply a pathological pressure gradient to the ventricular surface of the valve leaflets (Taramasso et al., 2012; Nickenig et al., 2017).

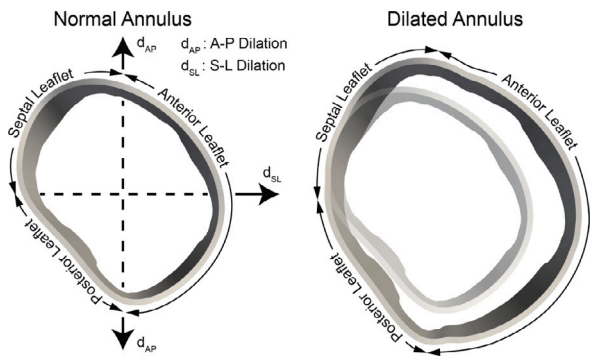

Fig. 2. Non uniform annular dilation. We dilate the healthy tricuspid annulus along the Anterior–Posterior (A–P) and Septal–Lateral (S–L) axes as observed in patients with pulmonary hypertension (Ring et al., 2012).
Source: Reproduced with permission from Mathur et al. (2022).

2.2. Remodeling-induced changes to the baseline valve model

To investigate the impact of remodeling-induced leaflet changes on valve mechanics, we alter three quantities as observed in our studies of remodeling tricuspid valves: (i) leaflet stiffness, (ii) leaflet thickness, and (iii) the stretch at which leaflets show strain-stiffening, which we subsequently call transition-λ. Previously, we have demonstrated that the tricuspid valve remodels in sheep with biventricular heart failure that develop tricuspid valve leakage. In those animals, we found that the anterior leaflet thickness increased by 40%, leaflet stiffness increased by 30%, and transition-λ decreased by 3%. Interested readers may find further details of our findings in our prior publication (Meador et al., 2020b). Please note that we did not observe any remodeling in the tricuspid chordae tendineae of sheep with functional tricuspid regurgitation. Thus, we have excluded such effects in our computational model.

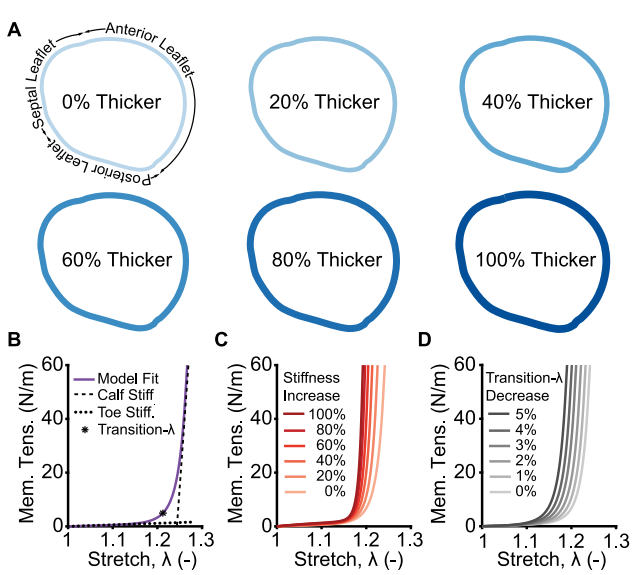

Fig. 3. Remodeling-induced macro- and micro-structural changes to the tricuspid valve. (A) Here, we uniformly increase leaflet thickness by 20%–100% in our simulations. (B) Furthermore, to alter the highly non-linear constitutive properties of the leaflets we first determine the slope of the tension–stretch curve at low and high stretch values, i.e. the toe- and calf-stiffness, respectively. Next, we identify the closest data point on the tension–stretch curve to the intersection of these slopes as the transition-λ. (C) We then simultaneously increase leaflet toe- and calf-stiffnesses by 20%–100% in our models. (D) Furthermore, we decrease leaflet transition-λ by 1–5%.

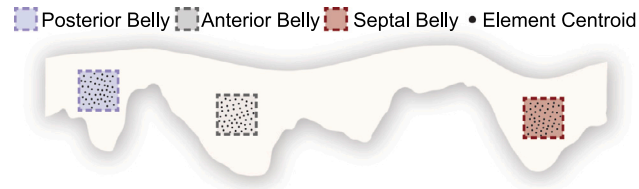

Fig. 4. Square regions where maximum principal Cauchy stresses are averaged for each tricuspid leaflet.

In this study, we first examine the sensitivity of our model to independent changes in leaflet thickness, stiffness, and transition-λ. Specifically, we increase leaflet thickness by 20%–100%, increase leaflet stiffness by 20%–100%, and finally decrease transition-λ by 1%–5%, as shown in Fig. 3. To quantify transition-λ, we first determine the slope of the leaflets' tension–stretch curve at low and high stretch values, i.e. the toe- and calf-stiffness, respectively. We then identify the closest data point on the tension–stretch curve to the intersection of these slopes as the transition-λ (Lin et al., 2022). See Tables A.1 and A.2 for altered stiffness and transition-λ values, respectively. We then examine the combined effects of remodeling-induced changes as observed in our previous sheep study. That is, we increase leaflet thickness by 40%, increase leaflet stiffness by 30%, and decrease transition-λ by 3%. To obtain the aforementioned values of leaflet thickness, leaflet stiffness, and transition-λ we modify the material parameters used in our computational model, as detailed in the online supplement to this article.

Furthermore, to quantify the impact of the remodeling-induced changes on valve function, we compare three metrics between all cases: (i) the average leaflet stress in leaflet centers, (ii) the leaflet systolic angle at end-systole, and (iii) the coaptation area. To average leaflet stresses, we first create a planar projection of the tricuspid leaflets, see Fig. 4. On this planar projection, we then create square regions of size 7 mm × 7 mm at the belly region of each tricuspid leaflet. Finally, for each tricuspid leaflet, we identify all element centroids within each square and compute the average maximum principal Cauchy stress (Haese et al., 2023).

3. Results

3.1. Isolated changes to leaflet thickness, stiffness, and transition-λ impact tricuspid valve function

To first study the "sensitivity" of the tricuspid valve to remodeling-induced leaflet changes, we separately study the leaflets' response to increased leaflet thickness and leaflet stiffness, and decreased transition-λ. Specifically, we first increased leaflet thickness by 20%–100%, before increasing leaflet stiffness by 20%–100%, and finally decreasing transition-λ by 1%–5%.

3.1.1. Impact on leaflet stresses

First, we investigated the impact of isolated remodeling-induced leaflet changes on leaflet stresses. To this end, we averaged leaflet stresses in a square region located in the center of each leaflet, see Fig. 5. We found that increasing leaflet thickness reduced average end-systolic stresses in each leaflet, see Fig. 5A. Specifically, increasing the leaflet thickness by 20%–100% led to a reduction in average stress of 23%–59% in the anterior, 18%–59% in the posterior, and 26%–61% in the septal leaflet. In contrast, we found that increasing leaflet stiffness increased average end-systolic stresses in each leaflet, see Fig. 5B. Here, we found that increasing leaflet stiffness by 20%–100% led to an increase in average stress of 9%–34% in the anterior, 5%–7% in the posterior leaflet, and 20%–154% in the septal leaflets. Finally, we found

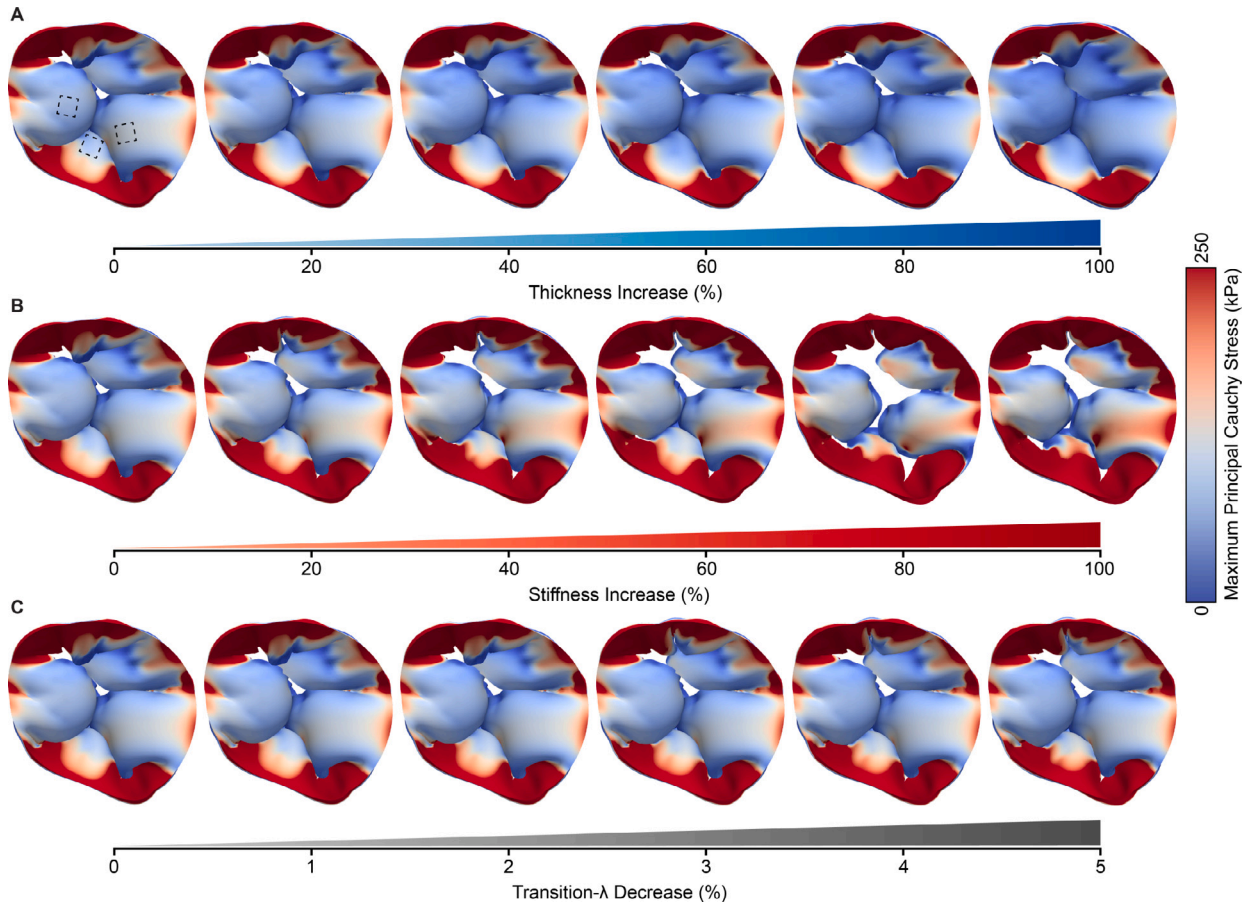

Fig. 5. Isolated remodeling-induced changes alter leaflet stresses in the regurgitant tricuspid valve. (A) Contours of stress overlaid on the end-systolic configuration of the tricuspid valve show that an isolated increase in leaflet thickness reduces leaflet stresses. In contrast, an isolated increase in stiffness or decrease in transition-λ increases leaflet stresses, as shown in (B) and (C), respectively. We compute average stresses for each leaflet in the regions indicated by a dashed square in (A).

Table 1
Leaflet stresses in the centers of tricuspid valve leaflets for the baseline valve with isolated changes to leaflet thickness, stiffness, and transition-λ. All values are presented as mean ± 1 S.D.

Condition	Change	Anterior leaflet		Posterior leaflet		Septal leaflet	
		Stress (kPa)	Change	Stress (kPa)	Change (%)	Stress (kPa)	Change (%)
Control	–	90.95 ± 25.25	–	65.88 ± 14.90	–	87.53 ± 32.74	–
Thickness increase	20%	70.19 ± 19.74	−22.82	53.92 ± 12.60	−18.17	64.36 ± 24.65	−26.47
	40%	60.15 ± 19.50	−33.87	44.14 ± 11.50	−33.01	57.71 ± 18.60	−34.07
	60%	49.49 ± 16.81	−45.59	36.26 ± 11.52	−44.97	41.15 ± 17.29	−52.99
	80%	44.95 ± 16.17	−50.57	32.48 ± 11.01	−50.70	41.67 ± 14.98	−52.40
	100%	37.64 ± 14.76	−58.61	27.05 ± 9.90	−58.95	33.90 ± 10.95	−61.28
Stiffness increase	20%	99.46 ± 30.92	9.37	69.29 ± 17.57	5.17	104.87 ± 43.09	19.81
	40%	107.35 ± 37.09	18.03	69.68 ± 20.45	5.76	132.46 ± 56.47	51.32
	60%	112.93 ± 43.35	24.17	69.19 ± 24.14	5.01	101.57 ± 45.74	16.04
	80%	105.47 ± 43.97	15.97	71.55 ± 26.68	8.59	187.31 ± 92.57	113.98
	100%	121.90 ± 54.81	34.04	70.39 ± 29.12	6.85	222.44 ± 115.69	154.12
Transition-λ decrease	1%	90.45 ± 24.53	−0.54	63.99 ± 14.03	−2.87	90.79 ± 34.22	3.72
	2%	89.11 ± 23.36	−2.02	63.58 ± 13.44	−3.50	97.81 ± 36.05	11.74
	3%	87.81 ± 22.83	−3.45	63.12 ± 12.84	−4.20	106.42 ± 38.37	21.57
	4%	87.86 ± 22.45	−3.39	62.56 ± 12.33	−5.05	115.06 ± 41.34	31.44
	5%	87.03 ± 22.29	−4.31	62.30 ± 11.94	−5.43	128.83 ± 46.79	47.18

that decreasing transition-λ altered average end-systolic stresses in each leaflet, see Fig. 5C. In detail, we found that decreasing transition-λ by 1%–5% led to a decrease in average stress of 1%–4% in the anterior leaflet and 3%–5% in the posterior leaflet. In contrast, average end-systolic stresses increased by 4%–47% in the septal leaflet. Leaflet stresses for the above cases are provided in Table 1. In summary, average end-systolic leaflet stresses are highly sensitive to changes in leaflet thickness, leaflet stiffness, and transition-λ.

3.1.2. Impact on leaflet systolic angle

Next, we investigated the impact of isolated remodeling-induced leaflet changes on the systolic angle of the anterior leaflet, see Fig. 6A. Additionally, we investigated the impact of isolated remodeling-induced leaflet changes on the leaflet contact area, i.e., coaptation area, see Fig. 6B.

Firstly, we found that increasing leaflet thickness reduced the anterior leaflet systolic angle, see Fig. 6C. Specifically, increasing the

Table 2
Anterior leaflet systolic angle and valve contact area for the baseline tricuspid valve as well as those values with isolated changes to leaflet thickness, stiffness, and transition-λ.

Condition	Change	Systolic angle (°)	Change (%)	Contact area (mm^2)	Change (%)
Control	–	10.77	–	251.64	–
Thickness increase	20%	8.73	−18.94	257.77	2.44
	40%	9.75	−9.52	271.30	7.82
	60%	8.13	−24.50	301.03	19.63
	80%	8.15	−24.37	287.71	14.34
	100%	5.72	−46.91	324.12	28.81
Stiffness increase	20%	14.13	31.11	132.51	−47.34
	40%	17.05	58.27	76.44	−69.62
	60%	18.63	72.91	70.28	−72.07
	80%	25.08	132.76	36.85	−85.36
	100%	21.44	99.03	22.53	−91.05
Transition-λ decrease	1%	11.20	3.94	229.96	−8.61
	2%	11.47	6.46	211.16	−16.08
	3%	11.94	10.86	176.33	−29.93
	4%	12.52	16.23	161.70	−35.74
	5%	13.16	22.20	134.84	−46.41

Table 3
Maximum principal Cauchy stresses in the central region of the baseline tricuspid valve (Control) as well as those valves with isolated and combined remodeling-induced changes. Specifically, a 40% increase in leaflet thickness, a 30% increase in stiffness, and a 3% decrease in transition-λ. All values are presented as mean ± 1 S.D.

Case	Condition	Anterior leaflet		Posterior leaflet		Septal leaflet	
		Stress (kPa)	Change (%)	Stress (kPa)	Change (%)	Stress (kPa)	Change (%)
I	Control	90.95 ± 25.25	–	65.88 ± 14.90	–	87.53 ± 32.74	–
IIa	Δ Thickness	60.15 ± 19.50	−33.87	44.14 ± 11.50	−33.01	57.71 ± 18.60	−34.07
IIb	Δ Stiffness	103.27 ± 34.83	13.55	72.65 ± 19.45	10.26	120.52 ± 49.50	37.68
IIc	Δ Transition-λ	87.81 ± 22.83	−3.45	63.12 ± 12.84	−4.20	106.42 ± 38.37	21.57
IIIa	Δ Thickness & Δ Stiffness	69.48 ± 28.64	−23.61	47.20 ± 15.88	−28.36	79.41 ± 27.80	−9.28
IIIb	Δ Stiffness & Δ Transition-λ	96.80 ± 28.45	6.44	65.73 ± 18.14	−0.23	129.25 ± 60.14	47.66
IIIc	Δ Transition-λ & Δ Thickness	57.96 ± 18.03	−36.27	43.02 ± 10.29	−34.71	71.72 ± 20.83	−18.07
IV	Combined Changes	67.41 ± 25.30	−25.88	47.74 ± 14.03	−27.55	102.71 ± 35.69	17.34

leaflet thickness by 20%–100% first led to a 19%–47% decrease in systolic angle at end-systole. In contrast, we found that increasing leaflet stiffness increased the anterior leaflet systolic angle, see Fig. 6D. In particular, we found that increasing stiffness by 20%–100% led to a 31%–133% increase in systolic angle at end-systole. Furthermore, we found that decreasing transition-λ increased leaflet systolic angles as well, as seen in Fig. 6E. That is, a 1%–5% decrease in transition-λ led to a 4%–22% increase in systolic angle at end-systole. Anterior leaflet systolic angles for the above cases are provided in Table 2. In summary, anterior leaflet systolic angles are highly sensitive to changes in leaflet stiffness and transition-λ but not leaflet thickness.

3.1.3. Impact on coaptation area

Secondly, we found that increasing leaflet thickness increased end-systolic coaptation area, see Fig. 6F. Specifically, increasing the leaflet thickness by 20%–100% led to a 2%–29% increase in coaptation area. In contrast, we found that increasing leaflet stiffness reduced end-systolic coaptation area, see Fig. 6G. In detail, increasing leaflet stiffness by 20%–100% led to a 47%–91% decrease in coaptation area. Finally, we found that decreasing transition-λ also reduced end-systolic coaptation area, see Fig. 6H. That is, a 1%–5% decrease in transition-λ led to a 9%–46% decrease in coaptation area. Leaflet contact areas for the above cases are provided in Table 2. In summary, leaflet contact areas are highly sensitive to changes in leaflet stiffness, leaflet thickness, and transition-λ.

3.2. Combined changes to leaflet thickness, stiffness, and transition-λ impact tricuspid valve function

In addition to studying the isolated effect of increasing leaflet thickness, increasing leaflet stiffness, and decreasing transition-λ, we also studied their combined effect. To this end, we chose values to match those observed in our previous sheep study (Meador et al., 2020b). Specifically, we combined a 40% increase in thickness with a 30% increase in stiffness and a 3% decrease in transition-λ.

3.2.1. Impact on leaflet stresses

Here, we introduced eight study cases to contrast the combined effect of remodeling-induced leaflet changes on valve function with their isolated impacts. A control case (I), cases investigating isolated changes only (II a/b/c), cases combining two of the leaflet changes (III a/b/c), and a final case in which we combine all changes (IV). In case IV we found that simultaneously increasing leaflet thickness and stiffness, and decreasing transition-λ by previously measured magnitudes led to a decrease in average stresses of 26% in the anterior and 28% in the posterior leaflets, see Fig. 7A. Additionally, this led to an increase in average stresses of 17% in the septal leaflet. As demonstrated by case IIIa, this response was driven by simultaneous changes in thickness and stiffness. Together, an increase in thickness and stiffness led to a decrease in average stresses of 24% in the anterior, 28% in the posterior leaflets, and 9% in the septal leaflet. Leaflet stresses for the above cases are provided in Table 3. In summary, the changes in average end-systolic leaflet stresses are driven by a simultaneous increase in leaflet thickness and stiffness.

3.2.2. Impact on systolic angle

Next, in case IV we found that remodeling-induced leaflet changes increase anterior leaflet systolic angle, see Fig. 7C. Specifically, a simultaneous increase in thickness and stiffness, and decrease in transition-λ led to a 43% increase in systolic angle. This change was primarily driven by an increase in stiffness, as exemplified by case IIb. Specifically, an increase in stiffness led to a 52% increase in systolic angle. Systolic angles for the above cases are provided in Table 4. In summary, the increase in systolic angles is primarily driven by an increase in leaflet stiffness.

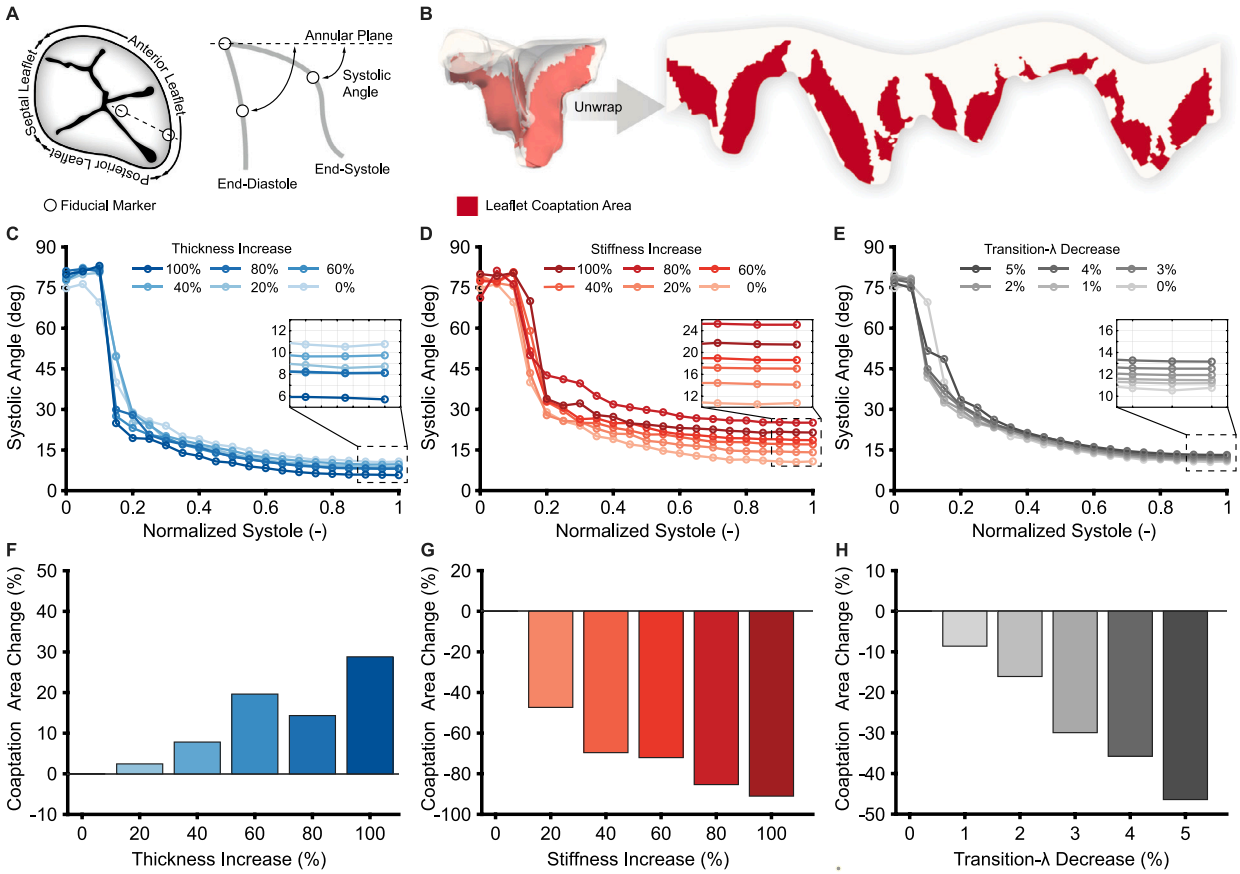

Fig. 6. Isolated remodeling-induced changes alter leaflet motion in the regurgitant tricuspid valve. (A) Here, we define the systolic angle as the angle between a point on the anterior leaflet and the annular plane during systole. (B) Furthermore, we quantify leaflet coaptation by considering the area of all finite-element faces in contact at end-systole, depicted here in red and projected on a 2D representation of the leaflet surface. (C) Increasing leaflet thickness non-uniformly decreases systolic angles. (D) In contrast, increasing leaflet stiffness substantially increases systolic angles. (E) Similarly, decreasing transition-λ increases systolic angles. (F) Here, we also see that an increase in leaflet thickness increases leaflet coaptation area. (G) In contrast, an increase in leaflet stiffness reduces leaflet coaptation area. (H) Finally, a decrease in transition-λ also decreases coaptation area.

3.2.3. Impact on coaptation area

Additionally, in case IV we found that remodeling-induced leaflet changes decrease leaflet coaptation area, see Fig. 7D. Specifically, a simultaneous increase in thickness and stiffness, and decrease in transition-λ led to a 66% decrease in coaptation area. This change was primarily driven by an increase in stiffness as seen in case IIb. To that end, an increase in stiffness by previously measured magnitudes led to a 59% decrease in coaptation area. Coaptation areas for the above cases are provided in Table 4. In summary, the decrease in leaflet contact areas is primarily driven by an increase in leaflet stiffness.

4. Discussion

Tricuspid valve leaflets have long been considered inert or "passive" structures. However, we recently demonstrated in sheep with functional tricuspid regurgitation that tricuspid valve leaflets may thicken, stiffen, and alter their material non-linearity. We hypothesize that these changes impede tricuspid valve coaptation and that suppressing them may restore valve function. The goal of our current work was to test this hypothesis, see Fig. 8.

In our first study, we examined the isolated effects of a remodeling-induced increase in thickness and stiffness as well as a decrease in transition-λ. We found that an isolated increase in leaflet thickness reduced stresses in the tricuspid valve. These computational findings agree with those of Kong and colleagues, who found a 40% decrease in leaflet stresses for a 62% increase in leaflet thickness (Kong et al., 2018). Additionally, we found that an isolated increase in leaflet stiffness increased stresses in the tricuspid valve. Kong et al. report a similar increase in stresses for stiffer tricuspid leaflets. Furthermore, we are the first to report that an isolated decrease in transition-λ increased leaflet stresses. While the sensitivity of leaflet stresses to transition-λ has never been directly investigated by others, in a computational model, Wu et al. observed that tricuspid valve stresses are highly sensitive to changes in leaflet constitutive properties (Wu et al., 2022). Next, we found that an isolated increase in stiffness and a decrease in transition-λ substantially increased anterior leaflet systolic angles. Interestingly, similar trends for leaflet stiffness were observed by others in a computer model of the regurgitant mitral valve (Wu et al., 2023). Finally, we found that an isolated increase in stiffness and decrease in transition-λ led to a decrease in coaptation area; thereby impacting valve function. While there are no similar studies for the tricuspid valve, others have previously observed such findings in computational models of the mitral valve (Kunzelman et al., 1998; Wu et al., 2023; Lee et al., 2015).

In our second study, we examined the combined effect of a remodeling-induced increase in thickness and stiffness as well as a decrease in transition-λ. We found reduced stresses in valves with thicker leaflets (case IIa) — even when accompanied by an increase in stiffness (case IIIa), decrease in transition-λ (IIIc), or both (case IV). This is likely due to the leaflets' folding resistance dominating their constitutive stiffness. That is, the leaflets increasingly resist folding and limit coaptation. As a result, the transvalvular pressure load is supported by a larger area. This, in turn, reduces inflation of the leaflets which decreases in-plane forces and reduces stresses. Next, we found that remodeling-induced changes, together (case IV), increase

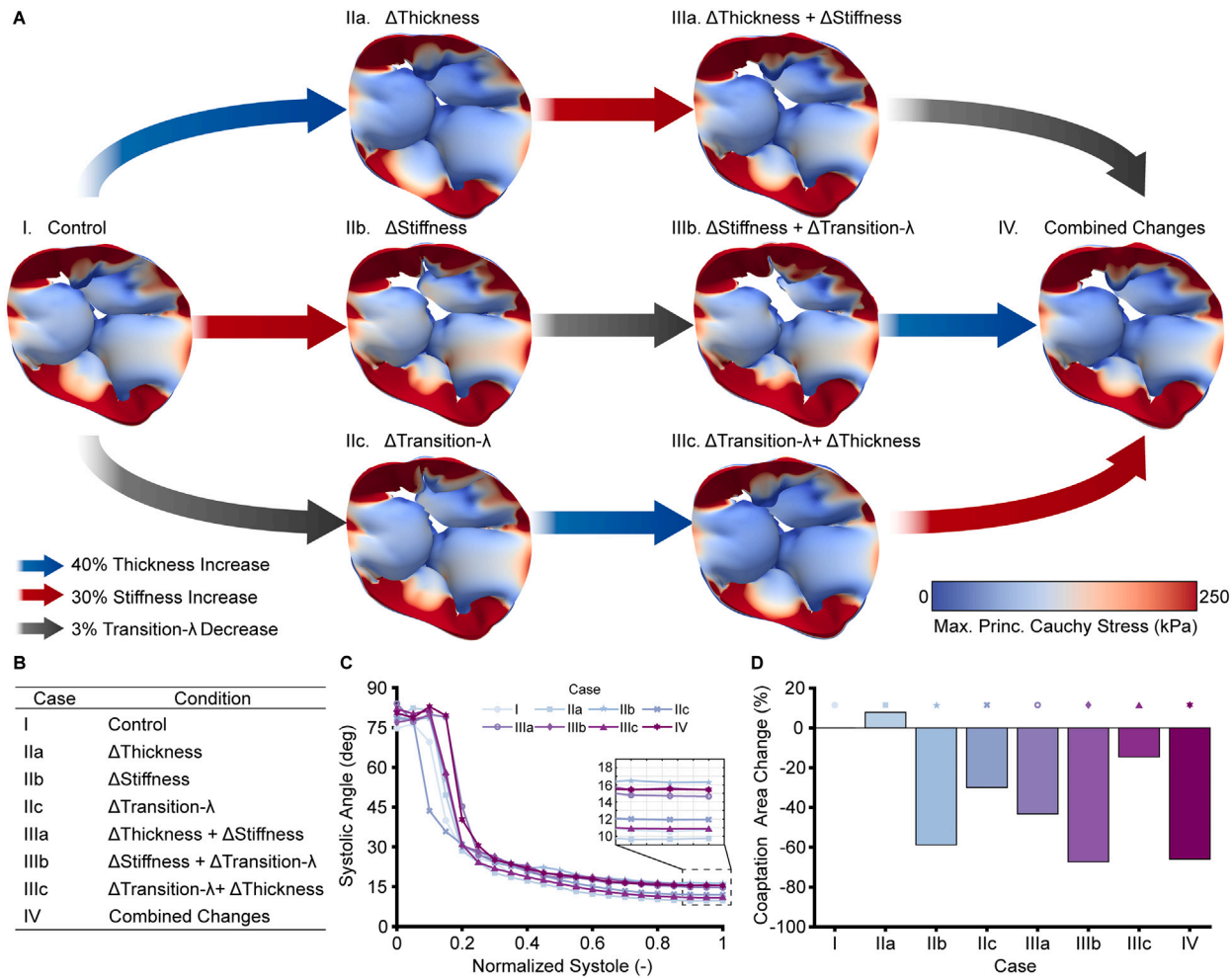

Fig. 7. Remodeling-induced changes alter leaflet stresses and motion in the regurgitant tricuspid valve. (A) Leaflet stresses in the tricuspid valve are sensitive to the combination of remodeling-induced changes in functional tricuspid regurgitation, as shown in (B). Similarly, changes to anterior leaflet systolic angles and valve coaptation area depend on the combination of remodeling-induced changes applied, as shown in (C) and (D), respectively.

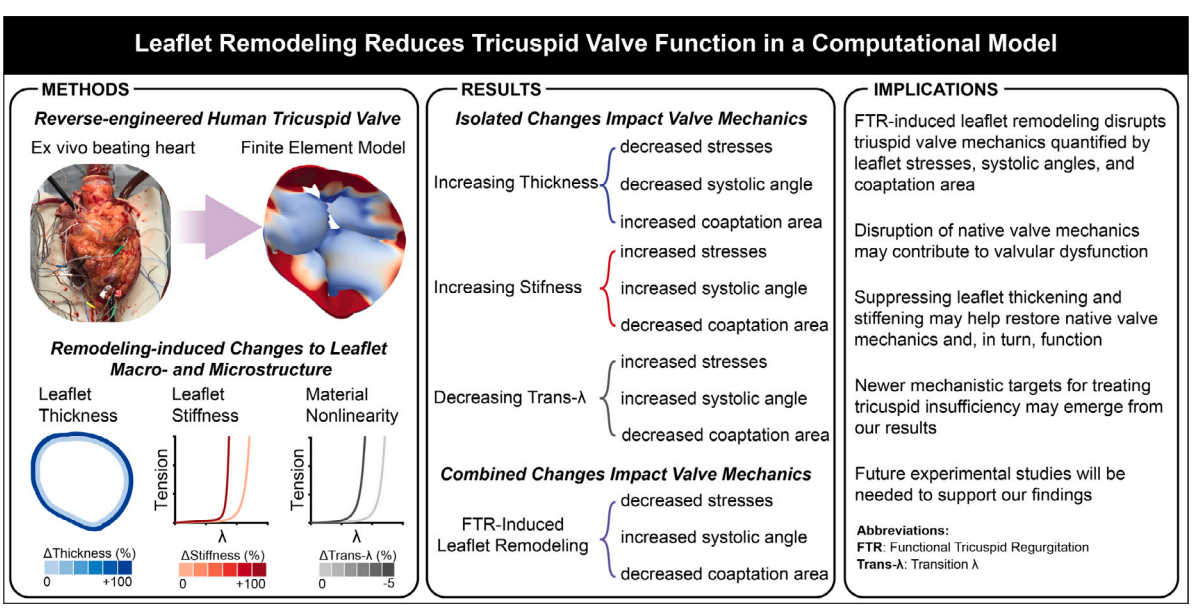

Fig. 8. We use a high-fidelity computational model of the human tricuspid valve to determine the impact of remodeling-induced changes to leaflet thickness, stiffness, and material nonlinearity. We found that these changes, both in isolation and when combined, impact leaflet stresses and motion. Thus, suppressing these changes may restore tricuspid valve function.

Table 4
Anterior leaflet systolic angle and valve contact area for the baseline tricuspid valve (Control) as well as those values with isolated and combined remodeling-induced changes. Specifically, a 40% increase in leaflet thickness, a 30% increase in stiffness, and a 3% decrease in transition-λ.

Case	Condition	Systolic angle (°)	Change (%)	Contact area (mm^2)	Change (%)
I	Control	10.77	–	251.64	–
IIa	Δ Thickness	9.75	−9.52	271.30	7.82
IIb	Δ Stiffness	16.32	51.51	103.70	−58.79
IIc	Δ Transition-λ	11.94	10.86	176.33	−29.93
IIIa	Δ Thickness & Δ Stiffness	14.66	36.03	142.90	−43.21
IIIb	Δ Stiffness & Δ Transition-λ	15.41	43.07	82.16	−67.35
IIIc	Δ Transition-λ & Δ Thickness	10.88	1.00	214.83	−14.63
IV	Combined Changes	15.44	43.28	85.51	−66.02

systolic angle. Notably, we previously observed a similar increase in experimentally measured anterior leaflet systolic angles in sheep with regurgitant valves (Jazwiec et al., 2021). Finally, we found that remodeling-induced changes, together (case IV), significantly decrease coaptation area. This implies that tricuspid valve function is negatively impacted. Furthermore, the coaptation area lost in a valve with a simultaneous increase in thickness and decrease in transition-λ (case IIIc) is less than a quarter of the coaptation area lost in the fully remodeled valve.

The significance of our findings is two-fold. Firstly, our findings may inspire novel, pharmacological strategies to treat functional tricuspid regurgitation (Rausch, 2020). For example, pharmaceutical treatments may be used to inhibit the thickening and stiffening of valve leaflets while permitting beneficial area growth. This strategy was successfully used by Bartko and colleagues to contain the fibrotic response of leaflets in the mitral valve in sheep. Specifically, they used Losartan, an angiotensin-II receptor blocker, to arrest an increase in leaflet thickness (Bartko et al., 2017). A similar strategy was used by Marsit et al. to reduce fibrotic thickening in ovine mitral leaflets using Cyproheptadine, a serotonin receptor 2B antagonist (Marsit et al., 2022). Secondly, our findings may be used to help understand the sub-optimal outcomes of surgical tricuspid valve repair. Specifically, we may better understand why some centers report failure rates as high as 25% within one year of patients being treated with the surgical gold standard — ring annuloplasty (Calafiore et al., 2019). In the porcine mitral valve, Sielicka and colleagues experimentally demonstrated that ring annuloplasty led to leaflet thickening and stiffening which, subsequently, resulted in valvular dysfunction (Sielicka et al., 2018). Suppressing similar changes due to tricuspid annuloplasty may, thus, improve valve function and repair outcomes.

Naturally, our study is subject to limitations. Firstly, we emulate leaflet remodeling as observed in a chronic model of functional tricuspid regurgitation in sheep. As such, inter-species differences as well as the gradual onset of disease may alter the extent of leaflet remodeling and its effects in patients. Secondly, we apply remodeling-induced changes observed in the centers of the ovine anterior leaflet to the posterior and septal leaflets. Furthermore, we homogenize these changes across the entire leaflet area. As such, we do not consider inter- and intra-leaflet variations in leaflet remodeling (Laurence et al., 2019). We hope future studies will elucidate these properties so that we may use them in subsequent models. Moreover, we represent the constitutive behavior of the tricuspid valve leaflets using a homogenized, isotropic strain energy function in our current finite element model. As such, we do not consider remodeling-induced changes in leaflet microstructure, as observed in our previous animal study (Meador et al., 2020b). To overcome this limitation, we hope to use a microstructurally-informed, anisotropic strain energy function to model the hyperelastic response of tricuspid valve leaflets in future releases of Texas TriValve (Sadeghinia et al., 2023). In addition to the above limitations, we may not generalize our results to all tricuspid valves due to the large variation in their leaflet morphology (Hahn et al., 2021). Last but not least, this is a computational study and caution is warranted.

5. Conclusions

In a virtual case study, we found that tricuspid valve function is sensitive to remodeling-induced leaflet changes. Specifically, leaflet stresses, anterior leaflet systolic angles, and valve contact area were all impacted by changes in leaflet thickness, leaflet stiffness, and material nonlinearity. Thus, these findings suggest that suppressing leaflet thickening and stiffening may, in fact, restore tricuspid valve function. In turn, our results may inspire novel surgical and pharmacological treatments for tricuspid regurgitation. Future experimental studies will be needed to support these findings.

CRediT authorship contribution statement

Mrudang Mathur: Writing – review & editing, Writing – original draft, Visualization, Software, Methodology, Investigation, Formal analysis, Data curation. **Marcin Malinowski:** Writing – review & editing, Writing – original draft, Methodology, Investigation. **Tomasz Jazwiec:** Writing – review & editing, Methodology, Investigation. **Tomasz A. Timek:** Writing – review & editing, Writing – original draft. **Manuel K. Rausch:** Writing – review & editing, Writing – original draft, Supervision, Project administration, Funding acquisition, Data curation, Conceptualization.

Declaration of competing interest

The authors declare the following financial interests/personal relationships which may be considered as potential competing interests: Manuel K. Rausch reports a relationship with Edwards Lifesciences Corporation that includes: speaking and lecture fees.

Data availability

The Abaqus input files for our tricuspid valve model are openly available through GitHub: https://github.com/SoftTissueBiomechanicsLab/Texas_TriValve.git.

Acknowledgments

This work was supported, in part, by the American Heart Association, United States of America through an award to Dr. Rausch (18CDA34120028) and a predoctoral fellowship to Mrudang Mathur (902502), as well as the National Institutes of Health, United States of America through awards to Dr. Rausch (1R21HL161832 and 1R01HL 165251). Additionally, we appreciate support from the National Science Foundation, United States of America through awards to Dr. Rausch (2127925, 2105175, 2046148, and 1916663) and the Office of Naval Research, United States of America through an award to Dr. Rausch (N00014-22-1-2073). Note, the opinions, findings, conclusions, or recommendations expressed are those of the authors and do not necessarily reflect the views of the American Heart Association, the National Institutes of Health, the Office of Naval Research, or the National Science Foundation. The authors also acknowledge the Texas Advanced Computing Center (TACC) at The University of Texas at Austin for providing high-performance computing resources that have contributed to the research results reported within this paper.

Table A.1
Toe- and calf-stiffness values identified for tricuspid valve leaflets under normal and stiffened material responses.

Stiffness	Anterior stiffness (N/m)		Posterior stiffness (N/m)		Septal stiffness (N/m)	
increase	Toe	Calf	Toe	Calf	Toe	Calf
0%	6.89	3046.50	9.02	3400.45	3.98	1881.91
20%	8.27	3655.72	10.82	4080.40	4.77	2258.17
40%	9.64	4264.97	12.63	4760.50	5.57	2634.53
60%	11.02	4874.28	14.43	5440.60	6.36	3010.95
80%	12.40	5483.59	16.24	6120.72	7.16	3387.39
100%	13.78	6093.00	18.04	6800.88	7.96	3763.89

Table A.2
Transition-λ values identified for tricuspid valve leaflets under normal and stiffened material responses.

Transition-λ decrease	Anterior transition-λ (–)	Posterior transition-λ (–)	Septal transition-λ (–)
0%	1.1524	1.1031	1.2613
1%	1.1409	1.0921	1.2486
2%	1.1294	1.0811	1.2362
3%	1.1179	1.0701	1.2234
4%	1.1064	1.0591	1.2110
5%	1.0948	1.0480	1.1982

Appendix A. Stiffness and transition-λ data

See Tables A.1 and A.2

Appendix B. Supplementary data

Supplementary material related to this article can be found online at https://doi.org/10.1016/j.jmbbm.2024.106453.

References

Afilalo, J., Grapsa, J., Nihoyannopoulos, P., Beaudoin, J., Gibbs, J.S.R., Channick, R.N., Langleben, D., Rudski, L.G., Hua, L., Handschumacher, M.D., Picard, M.H., Levine, R.A., 2015. Leaflet area as a determinant of tricuspid regurgitation severity in patients with pulmonary hypertension. Circ.: Cardiovasc. Imaging 8 (5), 1–8. http://dx.doi.org/10.1161/CIRCIMAGING.114.002714.

Badano, L.P., Muraru, D., Enriquez-Sarano, M., 2013. Assessment of functional tricuspid regurgitation. Eur. Heart J. 34 (25), 1875–1884. http://dx.doi.org/10.1093/eurheartj/ehs474.

Bartko, P.E., Dal-Bianco, J.P., Guerrero, J.L., Beaudoin, J., Szymanski, C., Kim, D.H., Seybolt, M.M., Handschumacher, M.D., Sullivan, S., Garcia, M.L., Titus, J.S., Wylie-Sears, J., Irvin, W.S., Messas, E., Hagège, A.A., Carpentier, A., Aikawa, E., Bischoff, J., Levine, R.A., 2017. Effect of losartan on mitral valve changes after myocardial infarction. J. Am. Coll. Cardiol. 70 (10), 1232–1244. http://dx.doi.org/10.1016/j.jacc.2017.07.734.

Calafiore, A.M., Foschi, M., Kheirallah, H., Alsaied, M.M., Alfonso, J.J., Tancredi, F., Gaudino, M., Di Mauro, M., 2019. Early failure of tricuspid annuloplasty. Should we repair the tricuspid valve at an earlier stage? The role of right ventricle and tricuspid apparatus. J. Card. Surg. 34 (6), 404–411. http://dx.doi.org/10.1111/jocs.14042.

Grande-Allen, K.J., Borowski, A.G., Troughton, R.W., Houghtaling, P.L., DiPaola, N.R., Moravec, C.S., Vesely, I., Griffin, B.P., 2005. Apparently normal mitral valves in patients with heart failure demonstrate biochemical and structural derangements. J. Am. Coll. Cardiol. 45 (1), 54–61. http://dx.doi.org/10.1016/j.jacc.2004.06.079.

Gupta, V., Grande-Allen, K.J., 2006. Effects of static and cyclic loading in regulating extracellular matrix synthesis by cardiovascular cells. Cardiovasc. Res. 72 (3), 375–383. http://dx.doi.org/10.1016/j.cardiores.2006.08.017.

Haese, C.E., Mathur, M., Lin, C.-Y., Malinowski, M., Timek, T.A., Rausch, M.K., 2023. Impact of tricuspid annuloplasty device shape and size on valve mechanics - a computational study. JTCVS Open 1–10. http://dx.doi.org/10.1016/j.xjon.2023.11.002.

Hahn, R.T., Weckbach, L.T., Noack, T., Hamid, N., Kitamura, M., Bae, R., Lurz, P., Kodali, S.K., Sorajja, P., Hausleiter, J., Nabauer, M., 2021. Proposal for a standard echocardiographic tricuspid valve nomenclature. JACC: Cardiovasc. Imaging 14 (7), 1299–1305. http://dx.doi.org/10.1016/j.jcmg.2021.01.012.

Iwasieczko, A., Gaddam, M., Gaweda, B., Goodyke, A., Mathur, M., Lin, C.-Y., Zagorski, J., Solarewicz, M., Cohle, S., Rausch, M., Timek, T.A., 2023. Valvular complex and tissue remodelling in ovine functional tricuspid regurgitation. Eur. J. Cardio-Thorac. Surg. 63 (5), ezad115. http://dx.doi.org/10.1093/ejcts/ezad115.

Jazwiec, T., Malinowski, M.J., Ferguson, H., Parker, J., Mathur, M., Rausch, M.K., Timek, T.A., 2021. Tricuspid valve anterior leaflet strains in ovine functional tricuspid regurgitation. Semin. Thorac. Cardiovasc. Surg. 33 (2), 356–364. http://dx.doi.org/10.1053/j.semtcvs.2020.09.012.

van Kelle, M.A., Rausch, M.K., Kuhl, E., Loerakker, S., 2019. A computational model to predict cell traction-mediated prestretch in the mitral valve. Comput. Methods Biomech. Biomed. Eng. 22 (15), 1174–1185. http://dx.doi.org/10.1080/10255842.2019.1647533.

Kong, F., Pham, T., Martin, C., McKay, R., Primiano, C., Hashim, S., Kodali, S., Sun, W., 2018. Finite element analysis of tricuspid valve deformation from multi-slice computed tomography images. Ann. Biomed. Eng. 46 (8), 1112–1127. http://dx.doi.org/10.1007/s10439-018-2024-8.

Kunzelman, K.S., Quick, D.W., Cochran, R.P., 1998. Altered collagen concentration in mitral valve leaflets: biochemical and finite element analysis. Ann. Thorac. Surg. 66 (6), S198–S205. http://dx.doi.org/10.1016/S0003-4975(98)01106-0.

Laurence, D., Ross, C., Jett, S., Johns, C., Echols, A., Baumwart, R., Towner, R., Liao, J., Bajona, P., Wu, Y., Lee, C.H., 2019. An investigation of regional variations in the biaxial mechanical properties and stress relaxation behaviors of porcine atrioventricular heart valve leaflets. J. Biomech. 83, 16–27. http://dx.doi.org/10.1016/j.jbiomech.2018.11.015.

Lee, C.-H., Rabbah, J.-P., Yoganathan, A.P., Gorman, R.C., Gorman, J.H., Sacks, M.S., 2015. On the effects of leaflet microstructure and constitutive model on the closing behavior of the mitral valve. Biomech. Model. Mechanobiol. 14 (6), 1281–1302. http://dx.doi.org/10.1007/s10237-015-0674-0.

Lin, C.-Y., Mathur, M., Malinowski, M., Timek, T.A., Rausch, M.K., 2022. The impact of thickness heterogeneity on soft tissue biomechanics: a novel measurement technique and a demonstration on heart valve tissue. Biomech. Model. Mechanobiol. 0–10. http://dx.doi.org/10.1007/s10237-022-01640-y.

Loerakker, S., Ristori, T., Baaijens, F.P., 2016. A computational analysis of cell-mediated compaction and collagen remodeling in tissue-engineered heart valves. J. Mech. Behav. Biomed. Mater. 58, 173–187. http://dx.doi.org/10.1016/j.jmbbm.2015.10.001.

Malinowski, M., Jazwiec, T., Goehler, M., Quay, N., Bush, J., Jovinge, S., Rausch, M.K., Timek, T.A., 2019. Sonomicrometry-derived 3-dimensional geometry of the human tricuspid annulus. J. Thorac. Cardiovasc. Surg. 157 (4), 1452–1461.e1. http://dx.doi.org/10.1016/j.jtcvs.2018.08.110.

Marsit, O., Clavel, M.-A., Paquin, A., Deschênes, V., Hadjadj, S., Sénéchal-Dumais, I., Couet, J., Arsenault, M., Handschumacher, M., Levine, R., Aikawa, E., Pibarot, P., Beaudoin, J., 2022. Effects of cyproheptadine on mitral valve remodeling and regurgitation after myocardial infarction. J. Am. Coll. Cardiol. 80, 500–510. http://dx.doi.org/10.1016/j.jacc.2022.05.025.

Mathur, M., Jazwiec, T., Meador, W.D., Malinowski, M., Goehler, M., Ferguson, H., Timek, T.A., Rausch, M.K., 2019. Tricuspid valve leaflet strains in the beating ovine heart. Biomech. Model. Mechanobiol. 18 (0123456789), 1351–1361. http://dx.doi.org/10.1007/s10237-019-01148-y.

Mathur, M., Meador, W.D., Malinowski, M., Jazwiec, T., Timek, T.A., Rausch, M.K., 2022. Texas TriValve 1.0 : a reverse-engineered, open model of the human tricuspid valve. Eng. Comput. http://dx.doi.org/10.1007/s00366-022-01659-w.

Meador, W.D., Mathur, M., Sugerman, G.P., Jazwiec, T., Malinowski, M., Bersi, M.R., Timek, T.A., Rausch, M.K., 2020a. A detailed mechanical and microstructural analysis of ovine tricuspid valve leaflets. Acta Biomater. 102, 100–113. http://dx.doi.org/10.1016/j.actbio.2019.11.039.

Meador, W.D., Mathur, M., Sugerman, G.P., Malinowski, M., Jazwiec, T., Wang, X., Lacerda, C.M., Timek, T.A., Rausch, M.K., 2020b. The tricuspid valve also maladapts as shown in sheep with biventricular heart failure. eLife 9, 1–22. http://dx.doi.org/10.7554/eLife.63855.

Muraru, D., Badano, L.P., 2022. Shedding new light on the fascinating right heart. Eur. Heart J. Cardiovasc. Imaging 23 (7), 863–866. http://dx.doi.org/10.1093/ehjci/jeac085.

Muresian, H., 2009. The clinical anatomy of the mitral valve. Clin. Anatomy 22 (1), 85–98. http://dx.doi.org/10.1002/ca.20692.

Nath, J., Foster, E., Heidenreich, P.A., 2004. Impact of tricuspid regurgitation on long-term survival. J. Am. Coll. Cardiol. 43 (3), 405–409. http://dx.doi.org/10.1016/j.jacc.2003.09.036.

Nickenig, G., Kowalski, M., Hausleiter, J., Braun, D., Schofer, J., Yzeiraj, E., Rudolph, V., Friedrichs, K., Maisano, F., Taramasso, M., Fam, N., Bianchi, G., Bedogni, F., Denti, P., Alfieri, O., Latib, A., Colombo, A., Hammerstingl, C., Schueler, R., 2017. Transcatheter treatment of severe tricuspid regurgitation with the edge-to-edge mitraclip technique. Circulation 135 (19), 1802–1814. http://dx.doi.org/10.1161/CIRCULATIONAHA.116.024848.

Pant, A.D., Thomas, V.S., Black, A.L., Verba, T., Lesicko, J.G., Amini, R., 2018. Pressure-induced microstructural changes in porcine tricuspid valve leaflets. Acta Biomater. 67, 248–258. http://dx.doi.org/10.1016/J.ACTBIO.2017.11.040.

Rausch, M.K., 2020. Growth and remodeling of atrioventricular heart valves: A potential target for pharmacological treatment? Curr. Opin. Biomed. Eng. 15, 10–15. http://dx.doi.org/10.1016/j.cobme.2019.12.008.

Rausch, M.K., Tibayan, F.A., Craig Miller, D., Kuhl, E., 2012. Evidence of adaptive mitral leaflet growth. J. Mech. Behav. Biomed. Mater. 15, 208–217. http://dx.doi.org/10.1016/j.jmbbm.2012.07.001.

Ring, L., Rana, B.S., Kydd, A., Boyd, J., Parker, K., Rusk, R.A., 2012. Dynamics of the tricuspid valve annulus in normal and dilated right hearts: A three-dimensional transoesophageal echocardiography study. Eur. Heart J. Cardiovasc. Imaging 13 (9), 756–762. http://dx.doi.org/10.1093/ehjci/jes040.

Sadeghinia, M.J., Aguilera, H.M., Urheim, S., Persson, R.M., Ellensen, V.S., Haaverstad, R., Holzapfel, G.A., Skallerud, B., Prot, V., 2023. Mechanical behavior and collagen structure of degenerative mitral valve leaflets and a finite element model of primary mitral regurgitation. Acta Biomater. 164, 269–281. http://dx.doi.org/10.1016/j.actbio.2023.03.029.

Sielicka, A., Sarin, E.L., Shi, W., Sulejmani, F., Corporan, D., Kalra, K., Thourani, V.H., Sun, W., Guyton, R.A., Padala, M., 2018. Pathological remodeling of mitral valve leaflets from unphysiologic leaflet mechanics after undersized mitral annuloplasty to repair ischemic mitral regurgitation. J. Am. Heart Assoc. 7 (21), 1–18. http://dx.doi.org/10.1161/JAHA.118.009777.

Taramasso, M., Vanermen, H., Maisano, F., Guidotti, A., La Canna, G., Alfieri, O., 2012. The growing clinical importance of secondary tricuspid regurgitation. J. Am. Coll. Cardiol. 59 (8), 703–710. http://dx.doi.org/10.1016/j.jacc.2011.09.069.

Wang, N., Fulcher, J., Abeysuriya, N., McGrady, M., Wilcox, I., Celermajer, D., Lal, S., 2019. Tricuspid regurgitation is associated with increased mortality independent of pulmonary pressures and right heart failure: A systematic review and meta-analysis. Eur. Heart J. 40 (5), 476–484. http://dx.doi.org/10.1093/eurheartj/ehy641.

Wang, H., Leinwand, L.A., Anseth, K.S., 2014. Cardiac valve cells and their microenvironment—insights from in vitro studies. Nat. Rev. Cardiol. 11 (12), 715–727. http://dx.doi.org/10.1038/nrcardio.2014.162.

Williams, T.H., Jew, J.Y., 2004. Is the mitral valve passive flap theory overstated? An active valve is hypothesized. Med. Hypotheses 62 (4), 605–611. http://dx.doi.org/10.1016/j.mehy.2003.12.001.

Wu, W., Ching, S., Maas, S.A., Lasso, A., Sabin, P., Weiss, J.A., Jolley, M.A., 2022. A computational framework for atrioventricular valve modeling using open-source software. J. Biomech. Eng. 144 (10), http://dx.doi.org/10.1115/1.4054485.

Wu, W., Ching, S., Sabin, P., Laurence, D.W., Maas, S.A., Lasso, A., Weiss, J.A., Jolley, M.A., 2023. The effects of leaflet material properties on the simulated function of regurgitant mitral valves. J. Mech. Behav. Biomed. Mater. 142, 105858. http://dx.doi.org/10.1016/j.jmbbm.2023.105858.